Journal of Structural Engineering & Applied Mechanics (2024) 7(1):34-50
DOI 10.31462/jseam.2024.01034050

RESEARCH ARTICLE

Using supplemental linear viscous dampers for experimentally verified base-isolated building: Case study

Adnan Kıral[1*], Ali Gurbuz[1]

[1] Recep Tayyip Erdogan University, Department of Civil Engineering, Rize, Türkiye

Article History

Received 10 December 2023
Accepted 25 March 2024

Keywords

Base isolation
Passive viscous damper
Earthquake
Seismic performance
Experimental results
MATLAB

Abstract

As a way to reduce structural vibration, many buildings are initially intended to be base-isolated. However, because of the base isolators' inherent nonlinear behavior, particularly in earthquake-prone areas, buildings equipped with base isolation systems may experience significant displacement demands. Therefore, in certain situations, it might be required to use additional damping devices to control the seismic response of base-isolated buildings. This study examines three different building models: Fixed Base (FB), Isolated Base (IB), and Isolated Base with installed Viscous Dampers (IB&VD) in the base layer of the building. Sosokan, a nine-story structure on Keio University's Yagami Campus, is utilized for this purpose. The building is modeled in MATLAB. A state-space representation of the building with a Maxwell-type viscous damper model is used. The responses of the building models with FB, IB, and IB&VD are evaluated by time history analyses using eight ground motion records. Certain engineering requirements criteria, such as inter-story drift ratios and absolute acceleration, are taken into consideration while evaluating the findings of the analysis. Based on one of this study's main findings, a base-isolated building with passive viscous damping in the base layer could significantly reduce both maximum seismic displacement and acceleration. Maximum acceleration and inter-story drift are lowered by up to 92% and 89%, respectively, when IB&VD is scaled to the FB model. Based on the results of this study, passive viscous dampers combined with building base isolation are not only useful for multi-objective optimization (i.e., reducing acceleration as well as inter-story drift) but they can also be used to reduce high-frequency accelerations, which could be important for building equipment that is sensitive to acceleration.

1. Introduction

Many lives and significant amounts of property have been lost because of the devastating earthquakes that have struck in recent years [2–4]. Seismic control technologies are becoming more and more crucial because of these losses. Recent advances in seismic isolation have led many developed countries, including Italy (2008), the USA (2009), Japan (2010), China (2010), Taiwan (2011), and Turkey (2018), to update their building regulations and encourage seismically isolated construction. Studies by Yurdakul et al. [5], Zhuang et al. [6], Sheikh et al. [7], Sesli et al. [8], and Losanno et al. [9] show that a great deal of effort has been

* Corresponding author (adnan.kiral@erdogan.edu.tr)
eISSN 2630-5763

made and is still being made to enhance the seismic response of structures using base isolators. "Elastomeric bearing systems" and "friction pendulum bearing systems" are the two basic isolation system types chosen in these studies. The function of a base isolation system is to isolate the structure from ground motion (especially the horizontal component of ground motion) by creating a layer of low horizontal stiffness between the structure and the foundation [10]. As elastomeric bearing systems, Natural and Synthetic Rubber Bearings (NRBs), Rubber Bearings (LRBs), or Lead Rubber Bearings (LRBs) are commonly used. A typical elastomeric bearing system with its hysteretic behavior is shown in Fig. 1.

Friction pendulum devices are mainly based on friction between stainless steel and Teflon. There are two basic types (flat and curved) of friction pendulums, depending on their sliding surface geometry. Researchers investigating the efficiency of friction-type base isolation systems claim that they may fail to restore themselves when seismic forces are applied [12]. For this reason, elastomer-bearing systems are preferred more often, especially in structures that are not very heavy [13]. Three common bearings are lead rubber bearings, friction pendulum bearings, and high-damping rubber bearings. Lead Rubber Bearing (LRB) is preferred due to its superior properties, as well as its resistance to corrosion and ease of maintenance. According to Cardone et al. [13], LRB lowered the maximum acceleration by around 20% on the floors of a six-story sample building. They also highlighted that the base isolation system significantly reduced building damage.

The base isolator increases the building period and reduces the acceleration values affecting the structure, but it can cause large displacements (especially in the isolation layer). Additionally, the deformation capacity of the isolator is limited under high displacement demands. Yaghmaei-Sabegh et al. [14] investigated the structural behavior of buildings with base isolation and claimed that if the duration of isolation increases the demand for inelastic displacement increases. Haiyang et al. [6] tried to evaluate the effect of LRBs by shaking table test, considering the structure-soil interaction. They found that during seismic events, a base-isolated structure's seismic responses are reduced due to soil-structure interaction. It should be noted that the presence of soft soil might allow ground vibrations to have a dominating period that is closer to the natural period of the base-isolated structure, potentially leading to structural resonance. Even though base isolation systems reduce the maximum acceleration values affecting the structure, they may not be seismically sufficient to protect the structure under strong earthquakes due to the large displacement demand from LRB, which might increase the pounding incidence with neighboring structures. Therefore, additional devices could be a solution to limit the relative story drifts and deformation of the LRB. Dampers, which can remove seismic energy from a building system, are widely adopted for this purpose in the literature on seismic control systems. Due to their high-energy dissipation capacity under dynamic loads, they are widely employed in the reduction of a structure's seismic response [15,16]. Various types of dampers, including metallic dampers, friction dampers, fluid viscous dampers, tuned mass dampers, etc., have been developed with different working principles. It is often chosen to use viscous dampers to create a system that works with base isolators and structures. Thanks to the fluid pressure inside that, they regulate the movement of the fluid by applying an opposing force proportional to the speed of the damper's movement. The general layout of a typical viscous damper is seen in Fig. 2a. A Maxwell-type damper model is shown in Fig. 2b.

The linear FVD damper force is expressed as follows:

$$F_d = C_d \, \dot{x} \, sign(x) \tag{1}$$

where F_d stands for the damper force C_d is the damping coefficient, x is the damper velocity, and $sign(x)$ is the signum function returning with +1 or -1.

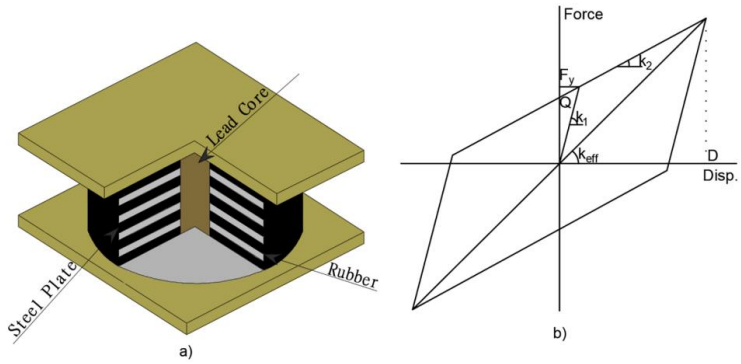

Fig. 1. Typical configuration and hysteretic behavior of LRB [11]

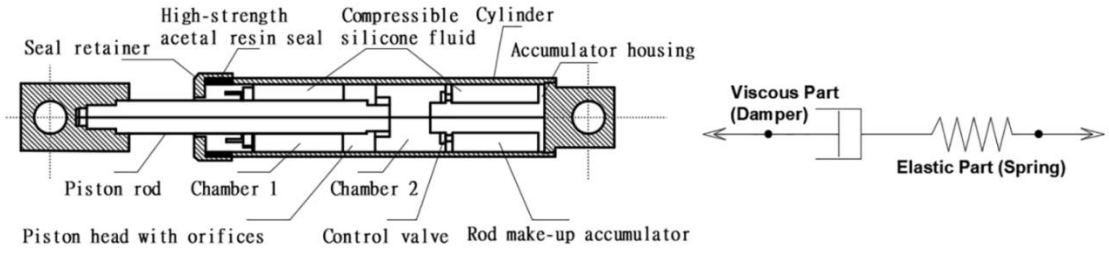

(a) (b)

Fig. 2. Typical FVD (a) outline and (b) Maxwell model [11]

Numerous studies have been conducted on the development of dampers, empirical validations, design improvements, and configuration of the layout of the fluid viscous damper. For example, Chalarca et al. [17] showed that the FVDs significantly reduced the floor acceleration response. They found that with the proper placement of FVDs, the maximum floor accelerations of the three-, six-, and nine-story sample structures could be lowered by 20% to 50%. Similarly, Tivari et al. [18] investigated the effect of viscous dampers on the earthquake performance of 5, 10, and 15-story sample buildings. They found that the maximum floor displacement of a 5-story building, which was equipped with viscous dampers, was decreased by approximately 50% compared to the reference structure. In the 10-story example building, displacements were reduced by around 25%, whereas in the 15-story example building, it was 20%. For a five-story base-isolated structure, Zhang and Iwan [19] evaluated the behavior of combining base isolation with FVDs. They observed that inter-story drifts may be significantly decreased using this type of system. They also suggested that an additional viscous damper would be more useful for the behavior of base-isolated buildings in terms of displacement of the isolation layer and acceleration at floor levels. Deringol and Guneyisi [11] investigated the effectiveness of FVD for a base-isolated 10-story steel moment-resisting frame isolated with LRB. They found that, especially under high-acceleration earthquakes, compared with buildings having only LRB, with the use of both LRB and FVDs on the isolated floor, the maximum story displacement of isolated frames was reduced from 10% to 25%.

This study discusses how much reduction is possible with each model (FB, IB, and IB&VD), as well as gives a reason for using viscous dampers for the benefit of reducing both seismic large displacements in the isolation layer and upper floors and reducing low- and high-frequency accelerations in a benchmark building. While acceleration reduction at low frequencies can be important for building occupants, high-frequency reduction can also be crucial for acceleration-sensitive equipment in buildings (e.g., museums, hospitals, or some special buildings). In this regard, this study demonstrates that adopting only base isolation systems

(i.e., no viscous dampers) may not achieve a desirable reduction in drift under strong earthquakes and accelerations in small earthquakes (or traffic movements, wind, etc.).

2. Numerical study

2.1. Adopted building

Completing its construction in 2000, Sosokan is a university building at Keio University (Fig. 3a) that has a base isolation system with passive viscous dampers installed in the base layer. Concrete-filled steel tubes, steel-reinforced concrete, and steel (as given in Table 1) make up the structure. There are nine levels in the building: one basement floor and eight stories above ground. The building's isolation layer plan is shown in Fig. 3b. Sixteen (16) passive hydraulic dampers aligned in the EW direction and sixty-five (65) laminated rubber bearings (LRBs), as given in Table 2, make up the isolation layer. Additionally, one of the viscous dampers placed in the building's isolation layer is depicted in Fig. 3c.

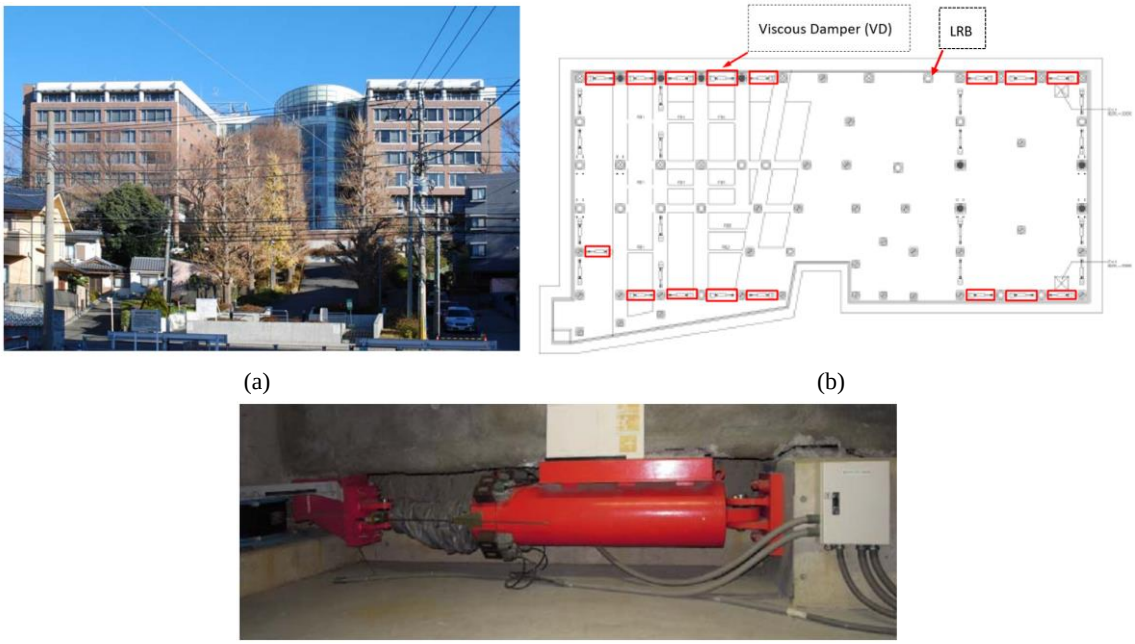

Fig. 3. (a) Facade of the Sosokan building, (b) isolation layer plan of the building, and (c) one of the existing viscous dampers in the building's isolation layer [1,20]

Table 1. The structural member details [1]

Member	Type of material	Type of geometry
Girders	Steel	H-(1000-600)×(300-200)×(12-22)×(19-40)
Member	Steel Steel-RC Concrete-filled steel tubes	B×D =1000×1000 Ø600, Ø550, Ø450

Table 2. The LRB properties [1]

Property	Isolator diameter				
	Ø1000	Ø900	Ø800	Ø700	Ø600
The number of isolators	8	10	15	20	12
Thickness and number of rubber layers	7.5 mm-26	6.8 mm-26	6.0 mm-26	5.3 mm-26	4.5 mm-33
Thickness and number of steel plates	4.5 mm-25	4.5 mm-25	4.5 mm-25	4.5 mm-25	3.2 mm-32
Upper and lower steel flanges	33 mm- Ø1450	32 mm-Ø1300	30 mm-Ø1200	25 mm-Ø1050	25 mm-Ø900
Anchor bolts	8-M42	8-M36	8-M36	8-M33	8-M33

2.2. Design and analysis of the adopted building

The building system's equation of motion is given by Dan and Kohiyama et al. [21] as follows:

$$\mathbf{M}\ddot{\mathbf{x}} + \mathbf{C}\dot{\mathbf{x}} + \mathbf{K}\mathbf{x} = \mathbf{E}\mathbf{u} + \mathbf{F}\ddot{\mathbf{z}} \tag{2}$$

with

$$\mathbf{x} = [x_1 \quad x_2 \quad \cdots \quad x_{10}]^{\mathrm{T}}$$

$$\mathbf{M} = \mathrm{diag}\,(m_1, m_2, \ldots, m_{10})$$

$$\mathbf{C} = \begin{bmatrix} c_1 + c_2 & -c_2 & \cdots & 0 & 0 \\ -c_2 & c_2 + c_3 & & & 0 \\ \vdots & & \ddots & & \vdots \\ 0 & & & c_9 + c_{10} & -c_{10} \\ 0 & 0 & \cdots & -c_{10} & c_{10} \end{bmatrix}$$

$$\mathbf{K} = \begin{bmatrix} k_1 + k_2 & -k_2 & \cdots & 0 & 0 \\ -k_2 & k_2 + k_3 & & & 0 \\ \vdots & & \ddots & & \vdots \\ 0 & & & k_9 + k_{10} & -k_{10} \\ 0 & 0 & \cdots & -k_{10} & k_{10} \end{bmatrix}$$

$$\mathbf{E} = [1 \quad \cdots \quad \cdots \quad 0]^{\mathrm{T}}$$

$$\mathbf{F} = [-m_1 \quad -m_2 \quad \cdots \quad -m_{10}]^{\mathrm{T}},$$

where mass, damping, and stiffness matrices are presented with M, C and K, respectively. The displacement vector, control force, and ground acceleration are denoted as x,u and ẗ, respectively.

The state space representation of Eq. (2) is also given as follows:

$$\dot{\mathbf{x}}_{\mathrm{t}} = \mathbf{A}\mathbf{x}_{\mathrm{t}} + \mathbf{B}u + \mathbf{D}\ddot{z} \tag{3}$$

where

$$\mathbf{x}_{\mathrm{t}} = \begin{bmatrix} \mathbf{x} \\ \dot{\mathbf{x}} \end{bmatrix}, \mathbf{A} = \begin{bmatrix} \mathbf{O}_{10\times10} & \mathbf{I}_{10\times10} \\ -\mathbf{M}^{-1}\mathbf{K} & -\mathbf{M}^{-1}\mathbf{C} \end{bmatrix},$$

$$\mathbf{B} = \begin{bmatrix} \mathbf{0}_{10\times1} \\ \mathbf{M}^{-1}\mathbf{E} \end{bmatrix}, \mathbf{D} = \begin{bmatrix} \mathbf{0}_{10\times1} \\ \mathbf{M}^{-1}\mathbf{F} \end{bmatrix}.$$

Including the Maxwell-type viscous damper model for the building system, the state equation is as follows:

$$\dot{\mathbf{x}}_{\mathrm{m}} = \mathbf{A}_{\mathrm{m}}\mathbf{x}_{\mathrm{m}} + \mathbf{B}_{\mathrm{m}}\tilde{u}_{\mathrm{s}} + \mathbf{D}_{\mathrm{m}}\ddot{z} \tag{4}$$

$$\mathbf{B}_u = [\mathbf{0}_{1\times 10} \quad 1 \quad \mathbf{0}_{1\times 9}] \tag{5}$$

with

$$\mathbf{x}_{\mathrm{m}} = \begin{bmatrix}\mathbf{x}_{\mathrm{t}} \\ x_{\mathrm{p}}\end{bmatrix} = \begin{bmatrix}\mathbf{x} \\ \dot{\mathbf{x}} \\ x_{\mathrm{p}}\end{bmatrix}, \mathbf{A}_{\mathrm{m}} = \begin{bmatrix}\mathbf{A} & -\mathbf{B} \\ k_{\mathrm{p}}\mathbf{B}_u & -\dfrac{k_{\mathrm{p}}}{c_{\mathrm{p}}}\end{bmatrix}, \mathbf{B}_{\mathrm{m}} = \begin{bmatrix}\mathbf{B} \\ 0\end{bmatrix}, \mathbf{D}_{\mathrm{m}} = \begin{bmatrix}\mathbf{D} \\ 0\end{bmatrix},$$

where $\tilde{u}_{\mathrm{s}}$ refers to the control force of a passive viscous damper. c_{p}, k_{p} and x_{p} denote the damping coefficient, stiffness, and displacement of the passive damper, respectively.

To model the building in MATLAB,

- The state space representation of the Sosokan building is defined as shown in Eqs. (3) and (4). The MATLAB's "ss" command, which creates a state-space model with given parameters (Table 3 and Table 4), is used.
- An earthquake data is saved in the MATLAB simulation file (one of the earthquake data given in Fig. 5).
- MATLAB's "lsim" command, which plots the simulated time response of the model, is employed. Note that MATLAB uses "Kernels for Linear Time-Invariant Systems".

Three building cases are modeled in MATLAB [22] such as

- Fixed Base (FB) refers to no base isolation in the model (i.e., nine-story building). For the model, eighteen-by-eighteen matrix sizes are used for mass (M), damping (C), and stiffness (K) in Eq. (3). In other words, k_1, c_1 and m_1 are excluded in the model matrixes. Because B2F (k_1, c_1 and m_1) is the isolation layer parameter.
- Isolated Base (IB) means that the model has a base isolation (i.e., a nine-story building with an isolation layer). For the model, a twenty-by-twenty matrix size is used for mass (M), damping (C), and stiffness (K) in Eq. (3).
- Isolated Base equipped with a Viscous Damper (IB&VD) refers to base isolation with installed viscous dampers in the isolation layer (i.e., a nine-story building with both having base isolation and installed viscous dampers at the same level). Eq. (4), which includes the Maxwell-type viscous damper model, is used for the model. The model has a twenty-one-by-twenty-one matrix size in mass (M), damping (C), and stiffness (K). Passive viscous damper parameters are also shown in Table 3.

B1F is the basement floor. The B2F level, which is given in Table 4, presents the base isolation layer. As expected, the stiffness and damping values on the B2F level are smaller than those on the other floors due to the isolation layer's low stiffness and damping values.

2.3. Building model verification

It is necessary to verify the code written in MATLAB before conducting building simulations. Therefore, by using Eq. (4) and given parameters in Table 3 and Table 4, the acceleration of 7F found in this study (Fig. 4a) is the same as the results given in Kohiyama et al [1], and Dan and Kohiyama [21] (Fig. 4b). Kohiyama et al. [1] discussed time history responses of the two Sosokan building models—one with structural parameters updated based on system identification (i.e., the design stage stiffness and damping coefficients of the building were updated by monitoring the building under several earthquakes; called "Updated") and the other with those at the design stage (called "Initial"). As shown in Fig. 4b, the outcomes were compared with the observation record (i.e., the acceleration records for the building were obtained from the sensors installed on the 7th floor; called "Record").

Table 3. Passive viscous damper parameters [21]

Stiffness	$\times 10^7$ N/m	Damping coefficient	$\times 10^7$ Ns/m
k_p	47.038	c_p	1.398

Table 4. Structural parameters of the building [1,21]

Floor	Mass $\times 10^6$ kg	Stiffness $\times 10^9$ N/m	Damping $\times 10^6$ Ns/m
RF	2.500	0.962	6.225
7F	2.066	1.203	7.777
6F	2.037	1.478	9.555
5F	2.037	1.807	11.687
4F	2.050	2.154	13.930
3F	2.033	1.975	12.773
2F	1.826	2.138	13.827
1F	2.491	2.930	18.946
B1F	3.439	2.232	14.437
B2F	4.981	0.104	0.000

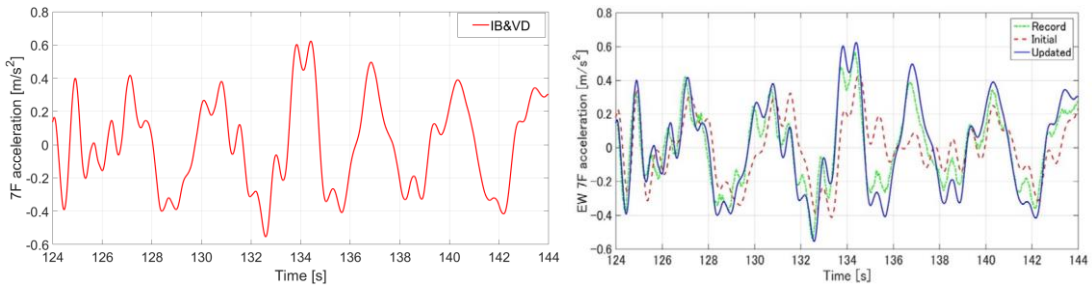

(a) (b)

Fig. 4. (a) The result of the IB&VD model found in this study and (b) 7F acceleration of Sosokan building given in Kohiyama et al. [1] for base isolated with sixteen viscous dampers (blue line, "Updated")

2.4. Seismic records

As part of their research for the Sosokan building, Kohiyama and Ito [23] synthesized 1000 simulated ground motions of "rare earthquake motion" and "very rare earthquake motion", which were prescribed in Notification No. 1461 of the Ministry of Construction, Japan, May 31, 2000. To generate waves with different ground motion intensities, parameters for wave amplitude envelope curves and design response spectra were linearly interpolated between the two previously described earthquakes. There was a range of 60 seconds to 120 seconds, and the PGV ranged from 0.0821 meters per second to 0.5643 meters per second. Only six of these generated records were investigated in this study, along with two natural ground motions (see Table 5, Fig. 5, and Fig. 6).

Table 5. Selected natural ground motion records

Source	Earthquake	Mw	Abbreviation	Station ID/component	PGA (g)
NOAA (2023)	2011 Tohoku	9.1	Tohoku	Tohoku/EW	0.711
PEER (2023)	1995 Kobe	6.9	Kobe	Takatori/TAK090	0.616

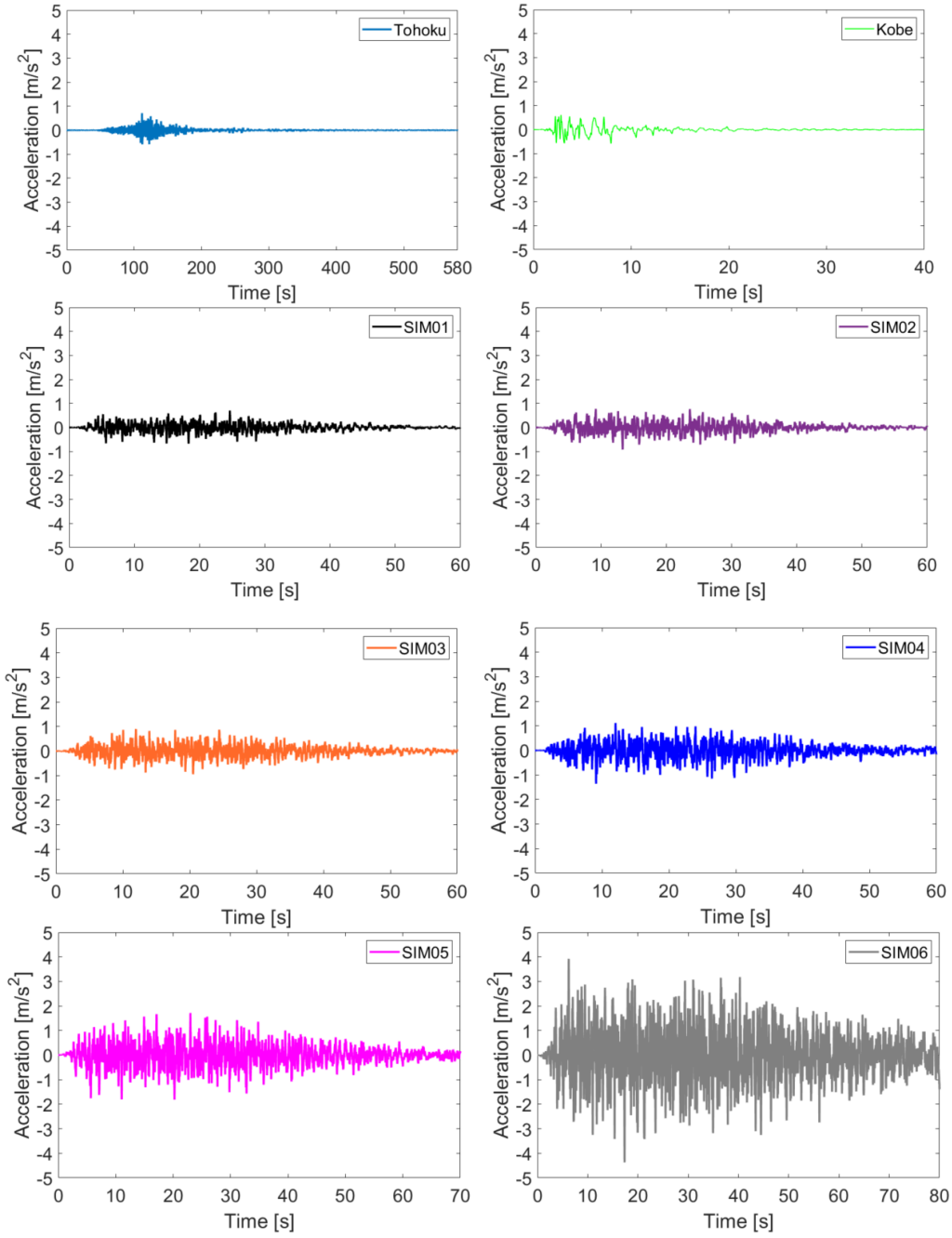

Fig. 5. Time history records of eight earthquakes

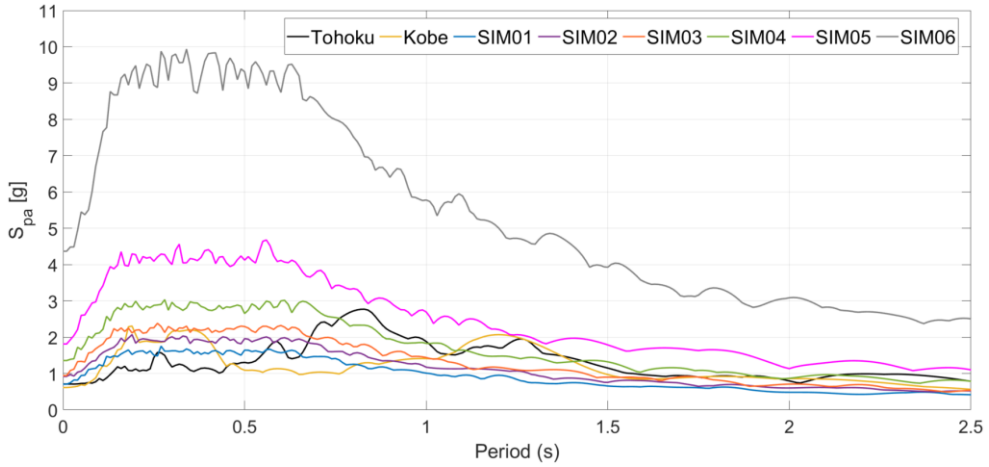

Fig. 6. 5% damped acceleration spectra of two natural and six generated earthquake records

3. Results and discussion

Three models (FB, IB, and IB&VD) were simulated under the Tohoku earthquake. Kohiyama et al. [1] stated that the Sosokan building had acceleration sensors, which were placed on the seventh floor (7F). To have consistency with the study [1], the time history acceleration of 7F was discussed in this study. From Fig. 7 and Table 6, the largest drift ratio (0.66%) and the biggest acceleration (3.41 m/s^2) of all three models were observed in the FB model. As the response of the other two models was scaled to FB, IB reduced the maximum inter-story drift and acceleration by 11% and 40%, whereas IB&VD resulted in 72% and 82% less, respectively. The results of IB&VD proved that it is possible to significantly reduce both inter-story drift and acceleration (Fig. 7 and Table 6). According to Fig. 7b, IB&VD can reduce both low- and high-frequency acceleration more effectively than the IB model. For buildings that have acceleration-sensitive equipment, high-frequency acceleration could be important. According to Fig. 7c, the IB&VD model reduced the maximum displacement of isolation level (B2F) by 72 percent compared to the IB model.

Under the Kobe earthquake, three models (FB, IB, and IB&VD) were simulated. FB model had the highest acceleration (3.82 m/s^2) and the biggest drift ratio (0.67%) of the three models, according to Fig. 8 and Table 6. After scaling the response of the other two models to FB, IB showed a reduction of 82% and 88% in maximum inter-story drift and acceleration, while IB&VD achieved a reduction of 89% and 92%, respectively. Inter-story drift and acceleration can be greatly reduced, as demonstrated by IB&VD results in Fig. 8 and Table 6. Fig. 8b shows that IB&VD is more effective than the IB model in reducing both the acceleration of low and high frequencies. High-frequency acceleration could be important for acceleration-sensitive equipment in buildings. Fig. 8c displays that the IB&VD model reduced the maximum displacement of isolation level (B2F) by 43 percent in comparison with the IB model.

FB, IB, and IB&VD models were simulated under the SIM01 earthquake. Fig. 9 and Table 6 show that among the three models, the FB model had the largest drift ratio (0.34%) and the biggest acceleration (1.97 m/s2). Following scaling the responses of the other two models to FB, IB showed a reduction in inter-story drift and acceleration of 33% and 59%, while IB&VD demonstrated a reduction of 79% and 84%, respectively. IB&VD results in Fig. 9 and Table 6 show that inter-story drift and acceleration can be significantly decreased. Fig. 9b shows how IB&VD can greatly reduce the acceleration of both low and high frequencies more effectively than the IB model. Equipment in buildings that is acceleration-sensitive could benefit from high-frequency acceleration reduction. When comparing the IB&VD model to the IB model, Fig. 9c shows that the maximum displacement of isolation level (B2F) is decreased by 72%.

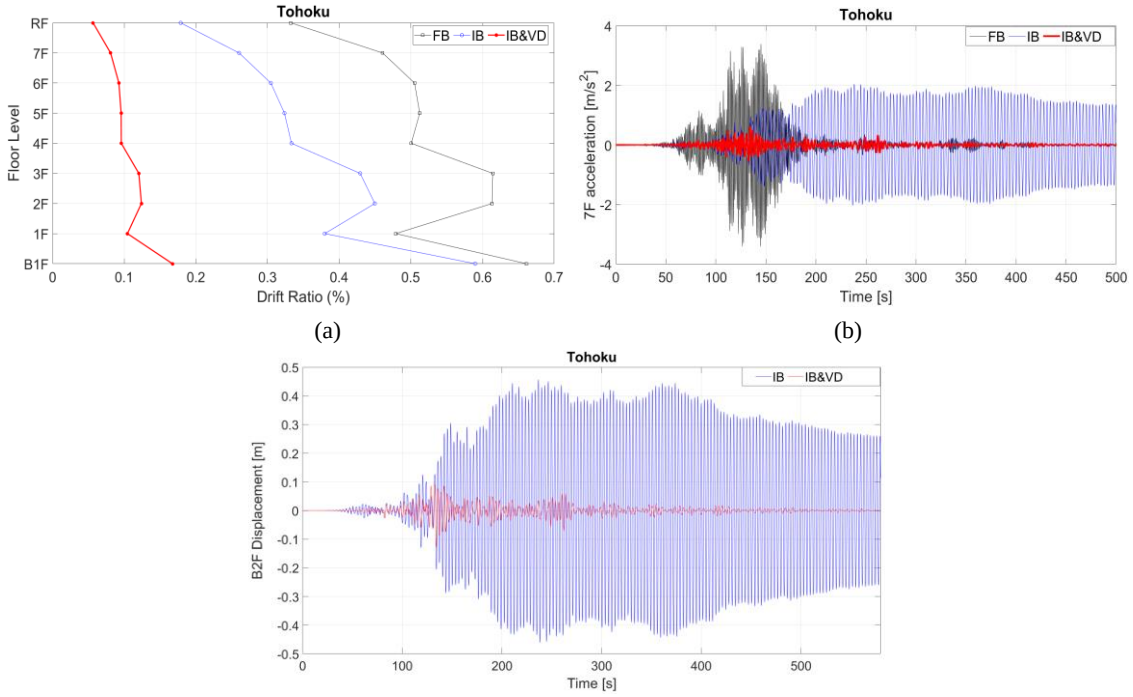

Fig. 7. The seismic response of FB, IB, and IB&VD models in terms of (a) maximum inter-story drift ratio, (b) time history of 7F acceleration, and (c) time history of isolation level (B2F) displacement under Tohoku earthquake

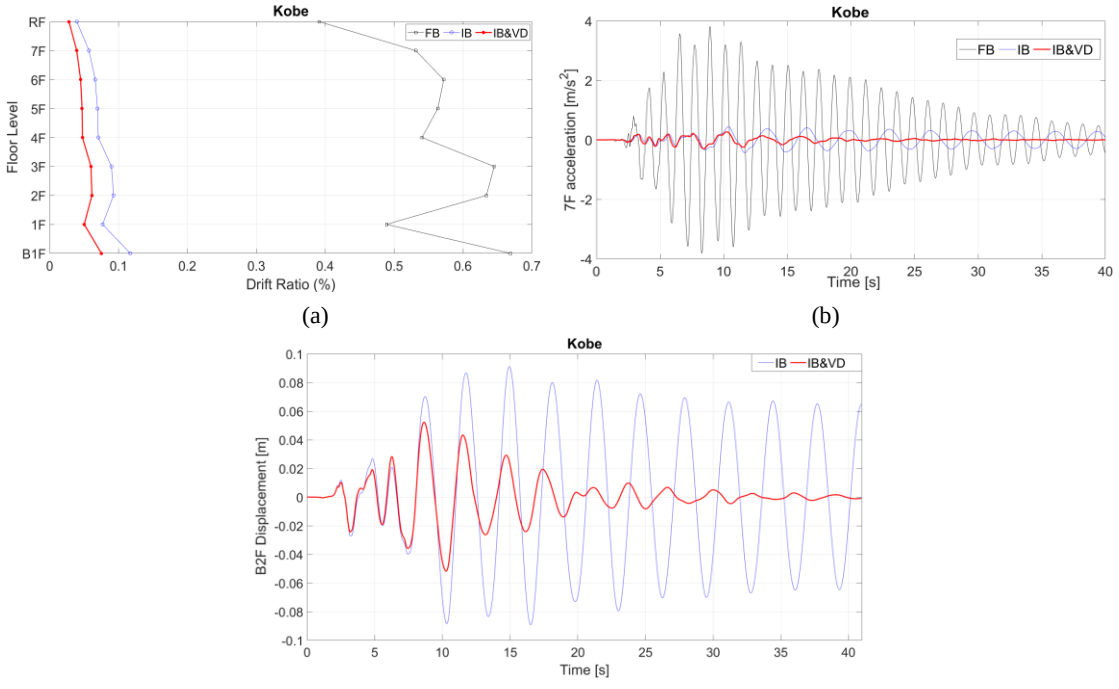

Fig. 8. The seismic response of FB, IB, and IB&VD models in terms of (a) maximum inter-story drift ratio, (b) time history of 7F acceleration, and (c) time history of isolation level (B2F) displacement under Kobe earthquake

Table 6. Main results of different models subjected to seismic records (Δ = reduction)

Record	Building Model	Max. 7F acceleration (m/s^2)	Δ	Max. inter-storey drift of the building (m)	Δ
Tohoku	FB	3.41	-	0.0198	-
	IB	2.05	-40%	0.0177	-11%
	IB&VD	0.62	-82%	0.0050	-72%
Kobe	FB	3.82	-	0.0201	-
	IB	0.44	-88%	0.0035	-82%
	IB&VD	0.30	-92%	0.0023	-89%
SIM01	FB	1.97	-	0.0102	-
	IB	0.81	-59%	0.0068	-33%
	IB&VD	0.32	-84%	0.0021	-79%
SIM02	FB	2.14	-	0.0098	-
	IB	1.04	-51%	0.0078	-20%
	IB&VD	0.43	-80%	0.0031	-68%
SIM03	FB	1.87	-	0.0114	-
	IB	1.27	-32%	0.0092	-19%
	IB&VD	0.42	-77%	0.0031	-73%
SIM04	FB	2.93	-	0.016	-
	IB	1.07	-63%	0.0082	-49%
	IB&VD	0.58	-80%	0.0043	-73%
SIM05	FB	5.24	-	0.0271	-
	IB	1.81	-65%	0.0130	-52%
	IB&VD	0.92	-82%	0.0057	-79%
SIM06	FB	11.34	-	0.0564	-
	IB	6.26	-45%	0.0541	-4.0%
	IB&VD	2.38	-79%	0.0131	-77%

SIM02 earthquake was used to simulate FB, IB, and IB&VD models. According to Fig. 10 and Table 6, the FB model had the highest acceleration (2.14 m/s2) and the largest drift ratio (0.33%) among the three models. IB showed a reduction in inter-storey drift and acceleration of 20% and 51%, whereas IB&VD achieved a reduction of 68% and 80%, respectively, after scaling the responses of the other two models to FB model. It is possible to significantly reduce the inter-story drift and acceleration, as demonstrated by the IB&VD results in Fig. 10 and Table 6. Compared to the IB model, Fig. 10b shows that IB&VD can reduce acceleration at both low and high frequencies more effectively. Building equipment that is sensitive to acceleration could find high-frequency acceleration mitigation useful. Fig. 10c illustrates that there is a reduction of 65% in the maximum displacement of isolation level (B2F) when comparing the IB&VD model to the IB model.

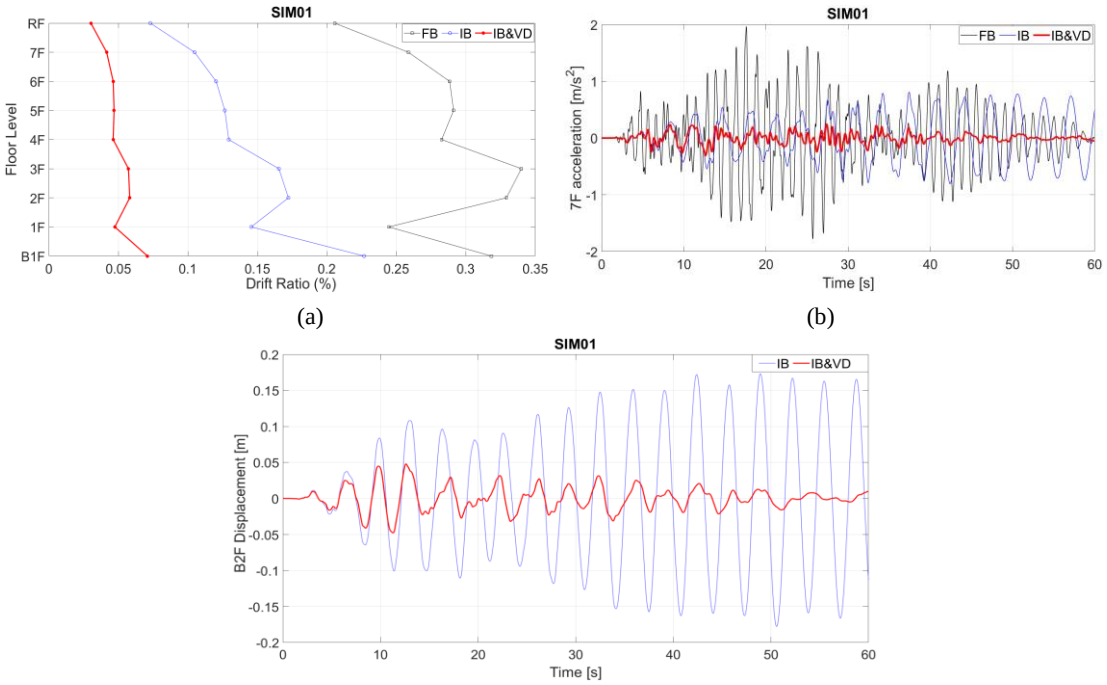

Fig. 9. The seismic response of FB, IB, and IB&VD models in terms of (a) maximum inter-story drift ratio, (b) time history of 7F acceleration, and (c) time history of isolation level (B2F) displacement under SIM01 earthquake

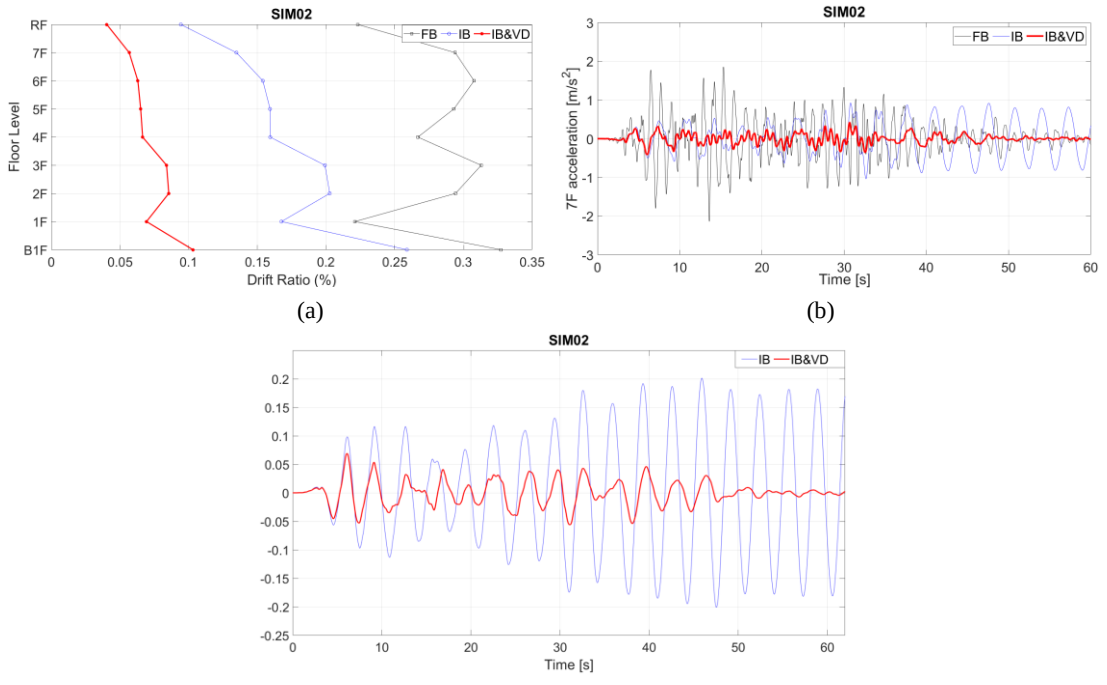

Fig. 10. The seismic response of FB, IB, and IB&VD models in terms of (a) maximum inter-story drift ratio, (b) time history of 7F acceleration, and (c) time history of isolation level (B2F) displacement under SIM02 earthquake

FB, IB, and IB&VD models were simulated using SIM03 record. Among the three models, the FB model resulted in the highest acceleration (1.87 m/s2) and the largest drift ratio (0.38%) (Fig. 11 and Table 6). After scaling the responses of the other two models to FB, IB showed a decrease of 19% and 32% in inter-story drift and acceleration, whereas IB&VD showed a reduction of 73% and 77%, respectively. Based on the IB&VD results shown in Fig. 11 and Table 6, inter-story drift and acceleration can be significantly reduced. Fig. 11b demonstrates that IB&VD is more successful at reducing acceleration at both low and high frequencies when compared to the IB model. High-frequency acceleration mitigation may be helpful in building equipment that is susceptible to acceleration. When the IB&VD model is compared to the IB model, the maximum displacement of isolation level (B2F) is reduced by 67%, as shown in Fig. 11c.

With the SIM04 record, FB, IB, and IB&VD models were simulated. Based on Fig. 12 and Table 6, the FB model resulted in the largest acceleration (2.93 m/s^2) and drift ratio (0.53%) of the three models. When comparing the inter-story drift and acceleration of the FB model with the other two models, IB demonstrated a reduction of 49% and 63%, respectively, while IB&VD demonstrated a reduction of 73% and 80%. Inter-story drift and acceleration can be considerably reduced by the IB&VD model (Fig. 12 and Table 6). In comparison to the IB model, Fig. 12b shows that IB&VD is more effective in reducing acceleration at both low and high frequencies. Equipment that is prone to acceleration may benefit from high-frequency acceleration mitigation. As Fig. 12c illustrates, there is a 52% reduction in the maximum displacement of isolation level (B2F) when the IB&VD model is compared to the IB model.

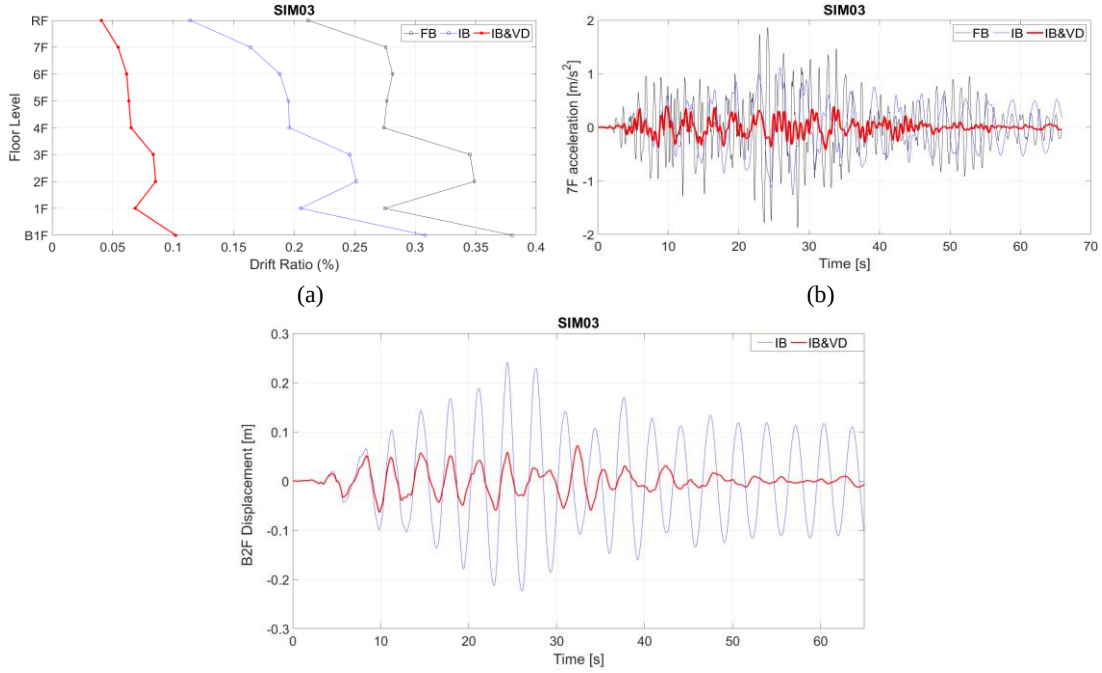

Fig. 11. The seismic response of FB, IB, and IB&VD models in terms of (a) maximum inter-story drift ratio, (b) time history of 7F acceleration, and (c) time history of isolation level (B2F) displacement under SIM03 earthquake

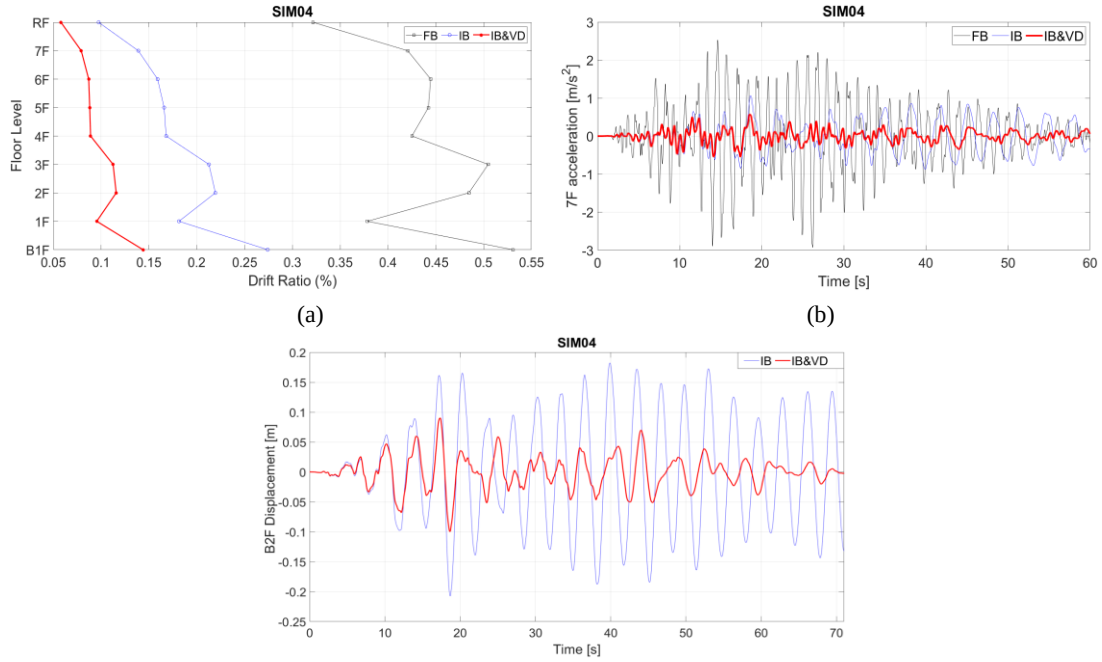

Fig. 12. The seismic response of FB, IB, and IB&VD models in terms of (a) maximum inter-story drift ratio, (b) time history of 7F acceleration, and (c) time history of isolation level (B2F) displacement under SIM04 earthquake

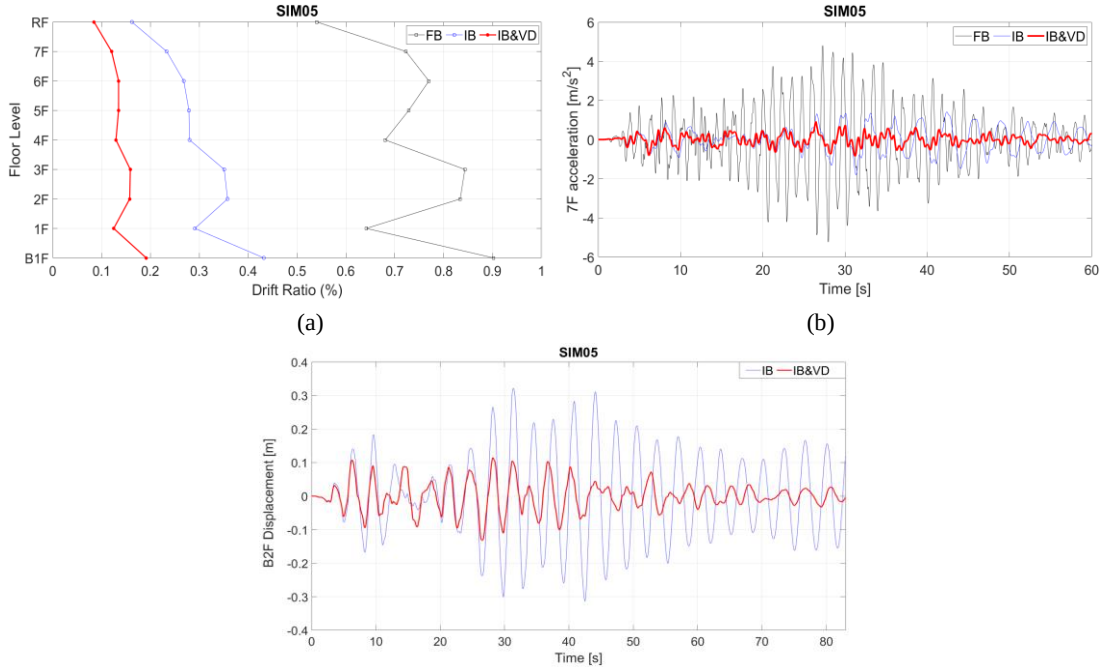

Fig. 13. The seismic response of FB, IB, and IB&VD models in terms of (a) maximum inter-story drift ratio, (b) time history of 7F acceleration, and (c) time history of isolation level (B2F) displacement under SIM05 earthquake

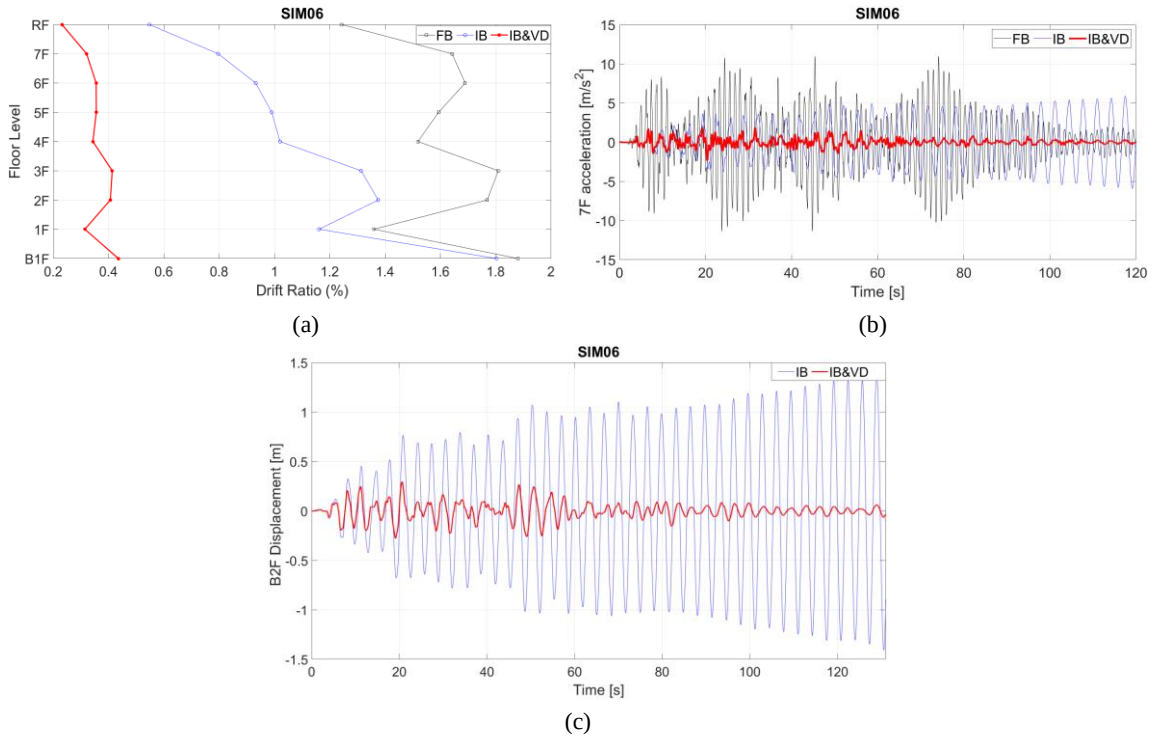

Fig. 14. The seismic response of FB, IB, and IB&VD models in terms of (a) maximum inter-story drift ratio, (b) time history of 7F acceleration, and (c) time history of isolation level (B2F) displacement under SIM06 earthquake

FB, IB, and IB&VD models were simulated using SIM05 records. Table 6 and Fig. 13 show that the FB model had the largest acceleration (5.24 m/s^2) and drift ratio (0.90%) of the three models. Compared with the FB model, IB showed reductions of 52% and 65%, respectively, in inter-story drift and acceleration, whereas IB&VD showed reductions of 79% and 82% (Table 6 and Fig. 13). The IB&VD model can significantly lower the inter-story drift and acceleration. Fig. 13b demonstrates that IB&VD is more effective at lowering acceleration at both low and high frequencies when compared to the IB model. Acceleration-prone equipment could benefit from high-frequency acceleration reduction. When comparing the IB&VD model to the IB model, the maximum displacement of isolation level (B2F) is reduced by 60%, as shown in Fig. 13c.

SIM06 record was used to simulate the FB, IB, and IB&VD models. Among the three models, FB exhibited the largest drift ratio (1.90%) and the biggest acceleration (11.34 m/s^2), as shown in Table 6 and Fig. 14. IB model demonstrated reductions in inter-story drift and acceleration of 4.0% and 45%, respectively, as compared to FB model, while IB&VD model demonstrated reductions of 77% and 79% (Table 6 and Fig. 14). The inter-story drift and acceleration can be considerably reduced using IB&VD model. In comparison to the IB model, Fig. 14b shows that IB&VD is more effective at reducing acceleration at both low and high frequencies. Reduced acceleration at high frequencies could be advantageous for building equipment that is prone to acceleration. The maximum displacement of isolation level (B2F) is lowered by 79% when comparing the IB&VD model to the IB model, as Fig. 14c shows.

4. Conclusions

The present study represents an analytical investigation of the responses of FB, IB, and IB&VD models under two recorded and six simulated earthquakes using MATLAB. A benchmark 9-story building, named

"Sosokan" in Japan, was considered for different building modeling. The IB&VD model used in this study was verified with the experimental results of Kohiyama et al. [1]. It was intended to investigate each building model's seismic response under different earthquakes and find one that could allow designers to consider multiple objective optimizations (e.g., acceleration and displacement). Based on the results of the analyses of eight earthquakes, the following conclusions can be drawn:

- The biggest absolute acceleration and the largest inter-story drift resulted in the FB model. The model's drift ratio and acceleration varied from 0.33% to 1.9% and 1.87 m/s2 to 11.34 m/s^2, respectively.
- The IB model outperformed FB by reducing the maximum acceleration varying from 32% to 88% and inter-story drift varying from 4% to 82%, yet the IB model can experience large drift under some earthquakes. Therefore, IB&VD could be a solution.
- The IB&VD model showed outstanding performance against FB and IB models. In comparison to FB, it reduced the maximum acceleration, which varied from 77% to 92%, and the inter-story drift, which varied from 68% to 89%. In addition, the IB&VD model reduced the acceleration at high frequencies apart from low frequencies. The reduction of acceleration at high frequencies could be beneficial for equipment that is prone to acceleration, such as museums, hospitals, or some special buildings.
- IB&VD model results may be used for developing more sophisticated building control systems (e.g., semiactive control) to further reduce both low- and high-frequency accelerations.

Acknowledgments

The first author acknowledges that this research, which was part of his Ph.D. studies, was made possible by a fully funded Ph.D. scholarship (2018-2022; Turkish law no. 1416 for the United Kingdom) provided by the Ministry of National Education of Türkiye. In addition, it is the first author's sincere gratitude to Professor Masayuki Kohiyama for providing technical assistance during his Japan visit (Keio University, 2019).

Conflict of interests

The author(s) declared no potential conflicts of interest with respect to the research, authorship, and/or publication of this article.

Data availability statement

Data generated during the current study are available from the corresponding author upon reasonable request.

References

[1] Kohiyama M, Omura M, Takahashi M, Yoshida O, Nakatsuka K (2019) Update of control parameters for semi-actively controlled base-isolated building to improve seismic performance. Japan Architectural Review 2(3):226–237.

[2] Gurbuz A, Tekin M (2017) Developing damage estimation methods for different types of reinforced concrete buildings. Technical Journal of Turkish Chamber of Civil Engineers 28(4):8051-8076. (in Turkish).

[3] Erturk E, Aykanat B, Altunısık AC, Arslan ME (2022) Seismic damage assessment based on site observation following the Düzce (Gölyaka) earthquake (Mw = 5.9, November 23, 2022). Journal of Structural Engineering & Applied Mechanics 5(4):197–221.

[4] Araz O, Kahya V (2018) Effects of manufacturing type on control performance of multiple tuned mass dampers under harmonic excitation. Journal of Structural Engineering & Applied Mechanics 1(3):117–127.

[5] Yurdakul M, Ates S, Tonyali Z (2017) Comparative study of non-isolated and isolated bridge with TCFP bearing under spatially varying ground motions. International Journal of Computational and Experimental Science and Engineering 3(2):29–32.

[6] Zhuang H, Fu J, Yu X, Chen S, Cai X (2019) Earthquake responses of a base-isolated structure on a multi-layered soft soil foundation by using shaking table tests. Engineering Structures 179:79–91.

[7] Sheikh H, Van Engelen NC, Ruparathna R (2022) A review of base isolation systems with adaptive characteristics. Structures 38:1542–1555.

[8] Sesli H, Tonyali Z, Yurdakul M (2022) An investigation on seismically isolated buildings in near-fault region. Journal of Innovative Engineering and Natural Science 2(2):47–65.

[9] Losanno D, Calabrese A, Madera-Sierra IE, Spizzuoco M, Marulanda J, Thomson P, Serino G (2022) Recycled versus natural-rubber fiber-reinforced bearings for base isolation: Review of the experimental findings. Journal of Earthquake Engineering 26(4):1921–1940.

[10] Ghorbi E, Toopchi-Nezhad H (2023) Annular fiber-reinforced elastomeric bearings for seismic isolation of lightweight structures. Soil Dynamics and Earthquake Engineering 166:107764.

[11] Deringol AH, Guneyisi EM (2021) Influence of nonlinear fluid viscous dampers in controlling the seismic response of the base-isolated buildings. Structures 34:1923–1941.

[12] Ponzo FC, Di Cesare A, Telesca A, Pavese A, Furinghetti M (2021) Advanced modelling and risk analysis of RC buildings with sliding isolation systems designed by the Italian Seismic Code. Applied Sciences 11(4):1–16.

[13] Cardone D, Conte N, Dall'Asta A, Di Cesare A, Flora A, Leccese G, Ragni L (2017) Rintc project: Nonlinear analyses of Italian code-conforming base-isolated buildings for risk of collapse assessment. In: Proceedings of COMPDYN 2017: 6th International Conference on Computational Methods in Structural Dynamics and Earthquake Engineering.

[14] Yaghmaei-Sabegh S, Safari S, Abdolmohammad-Ghayouri K (2017) Characterization of ductility and inelastic displacement demand in base-isolated structures considering cyclic degradation. Journal of Earthquake Engineering 23(4):557–591.

[15] Kelly JM, Konstantinidis DA (2011) Mechanics of Rubber Bearings for Seismic and Vibration Isolation. John Wiley & Sons Ltd.

[16] Jiang L, Zhong J, Yuan W (2020) The pulse effect on the isolation device optimization of simply supported bridges in near-fault regions. Structures 27:853–867.

[17] Chalarca B, Filiatrault A, Perrone D (2023) Influence of fluid viscous damper stiffness on the floor acceleration response of steel moment-resisting frames under far-field ground Motions. Journal of Earthquake Engineering 1–30.

[18] Tiwari P, Badal P, Suwal R (2023) Effectiveness of fluid viscous dampers in the seismic performance enhancement of RC buildings. Asian Journal of Civil Engineering 24(1):309–318.

[19] Zhang Y, Iwan WD (2002) Protecting base-isolated structures from near-field ground motion by tuned interaction damper. Journal of Engineering Mechanics 128(3):287–295.

[20] Dan M, Ishizawa Y, Tanaka S, Nakahara S, Wakayama S, Kohiyama M (2015) Vibration characteristics change of a base-isolated building with semi-active dampers before, during, and after the 2011 Great East Japan earthquake. Earthquake and Structures 8(4):889–913.

[21] Dan M, Kohiyama M (2013) System identification and control improvement of a semi-active-controlled base-isolated building using the records of the 2011 Great East Japan Earthquake. In Safety, Reliability, Risk and Life-Cycle Performance of Structures and Infrastructures. In: Proceedings of ICOSSAR: 11th International Conference on Structural Safety and Reliability

[22] MATLAB (2023) R2023a. Mathematical Computing Software for Engineers and Scientists. The MathWorks Inc., USA.

[23] Kohiyama M, Ito T (2014) Vibration controller design of a building–equipment system based on the seismic damage risk. In: Proceedings of Sixth World Conference on Structural Control and Monitoring, Barcelona, Spain.